7-21-2009

P2X antagonists inhibit styryl dye entry into hair cells

M. A. Crumling
University of Michigan Medical School

M. Tong
University of Michigan Medical School

K. L. Aschenbach
University of Michigan Medical School

L. Liu
University of Michigan Medical School

Published in final edited form as:
Neuroscience. 2009 July 21; 161(4): 1144–1153. doi:10.1016/j.neuroscience.2009.02.076.

P2X antagonists inhibit styryl dye entry into hair cells

Mark A. Crumling[1], **Mingjie Tong**[1], **Krista L. Aschenbach**[1,2], **Li Qian Liu**[1], **Christine M. Pipitone**[1], and **R. Keith Duncan**[1]

[1] Kresge Hearing Research Institute, Department of Otolaryngology, University of Michigan, Ann Arbor, MI 48109

[2] Calvin College, Grand Rapids, MI 49546

Abstract

The styryl pyridinium dyes, FM1-43 and AM1-43, are fluorescent molecules that can permeate the mechanotransduction channels of hair cells, the sensory receptors of the inner ear. When these dyes are applied to hair cells, they enter the cytoplasm rapidly, resulting in a readily detectable increase in intracellular fluorescence that is often used as a molecular indication of mechanotransduction channel function. However, such dyes can also permeate the ATP receptor, $P2X_2$. Therefore, we explored the contribution of P2X receptors to the loading of hair cells with AM1-43. The chick inner ear was found to express P2X receptors and to release ATP, similar to the inner ear of mammals, allowing for the endogenous stimulation of P2X receptors. The involvement of these receptors was evaluated pharmacologically, by exposing the sensory epithelium of the chick inner ear to 5 μM AM1-43 under different experimental conditions and measuring the fluorescence in hair cells after fixation of the tissue. Pre-exposure of the tissue to 5 mM EGTA for 15 minutes, which should eliminate most of the gating “tip links” of the mechanotransduction channels, deceased fluorescence by only 44%. In contrast, P2X receptor antagonists (PPADS, suramin, TNP-ATP, and d-tubocurarine) had greater effects on dye loading. PPADS, suramin, and TNP-ATP all decreased intracellular AM1-43 fluorescence in hair cells by at least 69% when applied at a concentration of 100 μM. The difference between d-tubocurarine-treated and control fluorescence was statistically insignificant when d-tubocurarine was applied at a concentration that blocks the mechanotransduction channel (200 μM). At a concentration that also blocks $P2X_2$ receptors (2 mM), d-tubocurarine decreased dye loading by 72%. From these experiments, it appears that AM1-43 can enter hair cells through endogenously activated P2X receptors. Thus, the contribution of P2X receptors to dye entry must be considered when using styryl pyridinium dyes to detect hair cell mechanotransduction channel activity in the absence of explicit mechanical stimulation of stereocilia.

Keywords

mechanotransduction; basilar papilla; auditory; AM1-43; FM1-43; pannexin

Styryl pyridinium (“styryl”) dyes, such as FM1-43, have been used classically to study the dynamics of endo- and exocytosis at synapses (Betz and Bewick, 1992, Betz et al., 1992, Choi

Correspondence should be addressed to: Mark A. Crumling, 9301 MSRB III, 1150 West Medical Center Dr. Ann Arbor, MI 48109-5648, Phone: 734-763-9680, Fax: 734-615-8111, Email: crumling@umich.edu.
Section Editor: **Sensory Systems**: Dr. Richard Weinberg, University of North Carolina, Department of Cell Biology and Anatomy, CB 7090, Chapel Hill, NC 27599, USA

et al., 2005) but are becoming increasingly popular as molecular markers of mechanotransduction channel function in hair cells, the sensory cells of the auditory and vestibular systems. These dyes are amphipathic molecules that can incorporate into vesicles and their membranes during the vesicle cycle (Betz et al., 1992). For examining the vesicle cycle, this endocytotic route is ideally the only means by which the dyes enter a cell. However, when applied to hair cells, the dyes enter the intracellular compartment not only in endocytosed vesicles (Meyer et al., 2001, Griesinger et al., 2002, 2004, Kaneko et al., 2006), but also through a faster, channel-mediated mechanism (Nishikawa and Sasaki, 1996, Gale et al., 2001, Meyers et al., 2003). There is compelling evidence that fast dye entry can occur via the hair cell transduction channels, which are located at the tips of the stereocilia (Gale et al., 2001, Meyers et al., 2003). Because of this, styryl dyes have been used as molecular markers of mechanotransduction channel activity in inner ear tissue (Geleoc and Holt, 2003, Si et al., 2003, Cheatham et al., 2004, Stepanyan et al., 2006, Taura et al., 2006, Spencer et al., 2008) and in experiments on the experimental manipulation of tissue to produce hair cells (Doyle et al., 2007, Hu and Corwin, 2007). However, rapid dye entry may not be a reliable indicator of transduction channel function. For example, differences in *in vitro* environment and species-specific factors could confound the ability to specifically associate rapid dye uptake with transduction channel function. This idea is supported by the disparity of dye loading mechanisms between guinea pig cochlear hair cells, where dye enters seemingly through endocytosis alone (Griesinger et al., 2002, 2004, Kaneko et al., 2006), and mouse, frog, chick, and fish hair cells, which show rapid, presumably channel mediated, dye entry (Nishikawa and Sasaki, 1996, Geleoc and Holt, 2003, Meyers et al., 2003, Si et al., 2003). Moreover, styryl dyes enter other types of sensory cells, apparently through non-specific cation channels that are distinct from that of the hair cell's transduction apparatus (Meyers et al., 2003). Since hair cells express many types of non-specific cation channels, fast dye loading may not only indicate transduction channel activity, but also the action of these other channels.

P2X receptors are extracellularly activated, ATP-gated, non-specific cation channels found in many cell types, including hair cells, where they are localized to the apical surfaces and stereocilia (Housley et al., 1992, Housley et al., 1998, Housley et al., 1999, Jarlebark et al., 2000). When these receptors are expressed in a cell line, FM1-43 rapidly enters the cells upon stimulation with ATP (Meyers et al., 2003). Likewise, stimulation of hair cells with ATP enhances their FM1-43 uptake (Ph.D. thesis, MacDonald, 2002). In the cochlea, there is a baseline presence of nanomolar concentrations of ATP in cochlear fluids. ATP is released in the cochlea during development (Tritsch et al., 2007), in response to intense noise exposure (Munoz et al., 2001), and by hypoxia (Munoz et al., 1995). Physical perturbation of the organ of Corti, as might occur during a dissection, is a robust means of inducing ATP release from supporting cells (Zhao et al., 2005). In light of the subcellular location of P2X receptors in hair cells and the endogenous presence of extracellular ATP in cochlear tissue, P2X receptors could partially mediate rapid styryl dye entry into hair cells, producing a spatial pattern similar to a transduction-mediated mechanism. Lending support to this idea, stimulation of P2X receptors in some cells confers permeability to large dye molecules (e.g., ethidium bromide and YO-PRO-1), thought to be due to dilation of the channel pore (Virginio et al., 1999, Chaumont and Khakh, 2008, Yan et al., 2008) or secondary activation of pannexin hemichannels (Pelegrin and Surprenant, 2006). Here, by using molecular and pharmacological techniques, we test the hypothesis that rapid styryl dye entry into hair cells can occur via a P2X-mediated mechanism.

Experimental Procedures

Tissue preparation for dye experiment

White leghorn chickens (*G. gallus*) were hatched in-house from embryonated eggs obtained from the Michigan State University Poultry Teaching and Research Center. Chicks, 5–10 days

post-hatch, were anesthetized with ketamine and xylazine (approximately 40 mg/kg and 10 mg/kg, respectively, via intramuscular injection) and decapitated. The temporal bone was opened, the partition between the round and oval windows was breached, and additional bone was dissected away so that the cochlea could be pulled out of its bony encasement. The cochleae were briefly treated (1 minute) with 0.01% protease dissolved in an artificial perilymph (AP) saline (in mM: 154 NaCl, 6 KCl, 5 $CaCl_2$, 2 $MgCl_2$, 5 HEPES, at pH 7.4) in order to facilitate further microdissection. After this treatment, the cochleae were transferred to a low-calcium Hanks' Balanced Salt Solution (LCHBSS: Gibco 14175 HBSS (Invitrogen) with 50 μM $CaCl_2$ added as 0.1 M $CaCl_2$). To improve reagent access to sensory hair cells, the tegmentum vasculosum and tectorial membrane were removed.

Dye treatment

Cochleae were kept in LCHBSS (control) or put in LCHBSS containing pharmacological agents before exposure to AM1-43 (pretreatment). In one set of experiments, a 15 minute pretreatment with 5 mM ethylene glycol-bis(2-aminoethylether)-*N*,*N*,*N*′, *N*′-tetraacetic acid (EGTA, Sigma) was used to disrupt tip links in order to inhibit dye entry through mechanotransduction channels. In experiments with P2X antagonists, a 5 minute pretreatment was used. The antagonists were pyridoxalphosphate-6-azophenyl-2′,4′-disulfonic acid (PPADS, Tocris Bioscience, 100 μM), suramin (Sigma, 100 μM), 2′,3′-O-(2,4,6-Trinitrophenyl) adenosine 5′-triphosphate (TNP-ATP, Sigma, 1 or 100 μM) and d-tubocurarine (Sigma, 200 μM or 2 mM). Additionally, 100 μM carbenoxolone (CBX, Sigma), an efficient blocker of gap junctions and related hemichannels, was used to test for dye entry through pannexin hemichannels using a 1 hour pretreatment. After pretreatment with a pharmacological agent or control saline, cochleae were exposed to LCHBSS with 5 μM AM1-43 (Biotium), a fixable analogue of FM1-43. The working dye solution was made from a concentrated stock solution daily. Except in the case of EGTA, the pharmacological agent used in the pretreatment was also present during the exposure to dye. The EGTA pretreatment solution was washed away with LCHBSS before exposing the tissue to dye. Exposure to the dye was for 1 minute, and it was immediately followed by three 30-second washes in LCHBSS containing 500 μM Advasep-7 (CyDex, Inc.) to remove stray AM1-43. After washing, cochleae were fixed (4% paraformaldehyde, 1 hour), washed in 0.12M phosphate buffer, and mounted on slides for fluorescence microscopy and digital imaging. The corresponding control tissues were handled similarly to the treated tissues, except for the omission of the pharmacological agent that was being tested.

Imaging and image analysis

The mounted tissue was viewed on a Leica DM LB fluorescence microscope. Images were acquired through a GFP filter with a cooled-CCD color digital camera (MicroPublisher, QImaging) using the same exposure settings for comparisons between drug and the corresponding non-drug control. AM1-43 fluorescence intensity in hair cells was quantified using MetaMorph image analysis software (Molecular Devices). Eliptical regions of interest (ROIs) that corresponded closely to the perimeter of individual hair cells were defined in the raw fluorescence images, and the fluorescence intensity within the ROIs was quantified in arbitrary units (Figure 1). When fluorescence intensity was below visual detection levels, ROIs were defined from transmitted light images. For each piece of tissue examined, the intensity of signal in 4 to 20 ROIs was averaged to give a value for that piece of tissue. This value was then averaged across all pieces of tissue subjected to a given experimental condition to give a mean ± standard error of the mean (SEM). The condition means were compared using an unpaired Student's t-test, and $p < 0.05$ was the criterion for statistical significance. For the images of AM1-43 loading, the only manipulations performed on the raw images were cropping, the addition of a scalebar and ROI labels, conversion to CMYK colorspace, and resizing.

ATP measurement

Cochleae were obtained as described above using the AP saline in place of LCHBSS. For each experiment, papillae were dissected, transferred to a microcentrifuge tube (2 papillae per tube), and incubated for 5 min in 200 μl of fresh AP. After this time period elapsed, the entire 200 μl of saline was collected and stored on ice. Fresh AP was added to the papilla samples, and the procedure was repeated for two more 5 minute intervals. Care was taken to perform solution exchanges without disturbing the tissue samples. Sterile reaction vessels and certified ATP-free plasticware were used throughout the procedures.

The concentration of ATP released from the cochlear samples ($[ATP]_o$) in each of the time intervals was measured with a single-tube luminometer (Cardinal Associates, Inc., Turner Model 20 Photometer) using a luciferin-luciferase ATP Assay Mix (FLAAM, Sigma-Aldrich). The assay mix was diluted 10-fold with dilution buffer. For each fluid sample, 100 μl of the diluted assay mix was added to a reaction vessel and allowed to sit at room temperature for 30 minutes while protected from light. After this time, an equal amount of fluid sample was added to the assay mix, swirled, and measured in the luminometer. The luciferin-luciferase reaction occurs quickly leading to a rapid decrease in the amount of light emitted over time. To limit variance due to differences in time between the mixing of solutions and measuring of luminescence, samples were placed in the luminometer precisely 20 seconds after mixing fluid samples with the assay mix. Standard curves were generated using ATP standards (Sigma-Aldrich) serially diluted in HPLC-grade water covering a concentration range of 20 pM to 2 nM ATP.

Estimate of local ATP concentration

The amount of ATP local to the release site (i.e., the basilar papilla) was estimated using a diffusion model. This model was developed for the experimental conditions described for the luciferin-luciferase assay and subsequently applied to the dye-labeling experiments to estimate the local concentration of ATP at the end of the one-minute dye incubation. The two basilar papillae in the luciferin-luciferase assay were approximated as a point source releasing ATP at a steady flux rate along a single dimension (i.e. the height of the reaction tube). This situation can be modeled by the one-dimensional diffusion equation for a semi-infinite domain (Mei, 1997), given by:

$$\frac{\partial c}{\partial t} = D\frac{\partial^2 c}{\partial x^2}, \quad 0 \le x \le \infty \qquad \text{(Eq. 1)}$$

where c is the concentration of ATP in moles per unit distance x at time t and D is the diffusion constant for ATP. A value of 700 $\mu m^2/s$ was chosen for D based on a previous report that experimentally determined the diffusion constant for Na_2ATP in water (Hazel and Sidell, 1987). The initial concentration of ATP at any point in the bulk solution was assumed to be zero, resulting in the initial condition $c(x,0) = 0$. Assuming the diffusion is rather limited compared with the height of the fluid column in the tube, we can assume a boundary condition of $c(\infty,t) = 0$. Since repeated samples from the same papillae gave relatively similar values of bulk ATP (see Results), we have modeled the release of ATP as a constant flux rate (A) at the point source, given by:

$$\frac{\partial c}{\partial x} = A, \quad \text{at } x=0, \qquad \text{(Eq. 2)}$$

Using these initial and boundary conditions, the solution to Equation 1 takes the form:

$$c(x,t) = -A\sqrt{\frac{D}{\pi}}\int_0^t \frac{e^{\frac{-x^2}{4D(t-\tau)}}}{\sqrt{t-\tau}}d\tau \quad \text{(Eq. 3)}$$

which can be solved to get the closed-form solution:

$$c(x,t) = A^*\left(\sqrt{\frac{4Dt}{\pi}} * e^{\frac{-x^2}{4Dt}} - x^* erfc\left(\frac{x}{\sqrt{4Dt}}\right)\right) \quad \text{(Eq. 4)}$$

The concentration of ATP in bulk solution after 5 minutes (see Results) was about 1 nM for two papillae submerged in a fluid volume of 200 μl. A value for the flux rate, *A*, was determined by integrating concentration and equating this to the total amount of ATP in the bulk solution, or:

$$\int_0^\infty c\,dx = 200\,fmol \quad \text{(Eq. 5)}$$

The numerical integration of Equation 5 at the 5-minute time point allowed us to determine *A* as 9.55×10^{-19} moles/μm^2.

P2X and Pannexin expression analysis

Cochlear tissue samples were harvested as described above, treated with protease, and microdissected in AP to expose the sensory epithelium. All procedures were conducted under RNase free conditions. Sensory epithelia, consisting of hair cells and supporting cells, were dissected free from the basilar membrane and transferred to RLT extraction buffer with β-mercaptoethanol (Qiagen). RNA from accessory tissues disrupted during the dissection is probably transferred along with the sensory epithelia. To account for the contribution of this RNA, dissection saline was sampled after removal of the epithelia and tested in parallel with tissue samples. Total RNA was extracted and purified using RNeasy Micro Kits (Qiagen). Reverse-transcribed cDNA was synthesized from 1–5 μg of total RNA using SuperScript III reverse transcriptase according to the manufacturer's instructions (Invitrogen). The first-strand synthesis reaction was performed at 50°C for 60 minutes, then inactivated at 70°C for 15 minutes.

PCR reactions were performed with 100–500 ng template cDNA in the presence of 2.5 U of Platinum Taq DNA polymerase (Invitrogen), 2 _mM $MgCl_2$, 0.2 mM dNTP mix (Invitrogen), 0.2 μM of each primer, and enough magnesium-free PCR buffer to reach a reaction volume of 50 μl. Amplification was performed in a thermal cycler (Mastercycler, Eppendorf) over 35 cycles following an initial denaturing step to 94°C for 5 minutes and concluding with an extension for 10 minutes at 72°C. Each cycle included a step to 94°C for 45 seconds (denature), a step to 60°C for 45 seconds (anneal), and a step to 72°C for 2 minutes (extension). PCR primers (Table 1) were designed using Primer3 0.4.0 web-based software (http://frodo.wi.mit.edu/) and synthesized by Invitrogen. PCR products were electrophoresed on a 1.0% agarose gel and digitally imaged to determine size. The gel images are brightness-inverted for presentation.

Results

AM1-43 rapidly entered hair cells of the chick basilar papilla, robustly labeling these cells during a 1 minute exposure to the dye. The exemplar image in Figure 1 is taken at the level of

hair cell nuclei from a region along the inferior edge of the basilar papilla. Dye label was excluded from the nucleus and interstitial supporting cells while effectively labeling the cytoplasm of hair cells. Loading the cytoplasm with dye on such a short time scale suggests permeation through channels (Gale et al., 2001,Meyers et al., 2003), rather than uptake via ongoing endocytosis (Meyer et al., 2001,Griesinger et al., 2002,2004). The variance in this plot represents the standard error of the mean fluorescence within a single basilar papilla. The mechanism behind this variable uptake of dye in a single piece of tissue is unclear, but it may be attributed to a nonuniform distribution, activation, or functionality of channels that mediate dye influx. Care was taken to measure fluorescence of hair cells throughout the papilla, covering the full range of intensities present in the tissue. The data throughout the remainder of this paper represent averages of the mean fluorescence from individual papillae.

The mechanosensitive transduction channels represent one pathway through which styryl dyes can rapidly enter hair cells (Nishikawa and Sasaki, 1996, Gale et al., 2001, Meyers et al., 2003). Tip links are fine filamentous linkages between stereocilia and are believed to mechanically gate the hair cell transduction channels (for review of transduction, see Vollrath et al., 2007). Destruction of tip links with the calcium chelators, EGTA or BAPTA, abolishes macroscopic transduction responses (Marquis and Hudspeth, 1997) and therefore should be an effective means of preventing rapid dye loading through this avenue. Pretreatment of the chick basilar papilla with 5 mM EGTA decreased loading of hair cells with AM1-43, although the block was incomplete (Figure 2A and B). Exposure of turtle hair cells to solutions containing the calcium chelators, HEDTA or BAPTA, at 5 mM concentration leaves about two transduction channels still able to gate (Crawford et al., 1991, Ricci et al., 2003). The same might be expected to occur in chick auditory hair cells, where 2 mM EGTA decreases the number of identifiable tip-links by 86% (Duncan et al., 1998). Yet, AM1-43 fluorescence intensity decreased to just over half the level seen in control tissue treated similarly without the addition of EGTA. This result is comparable to a previous report using treatment with the tip link breaker, BAPTA (5 mM), to block FM1-43 uptake in frog saccular hair cells (Meyers et al., 2003). One possible explanation is that a modicum of surviving tip links after EGTA treatment is capable of allowing substantial dye accumulation. Another possibility is the existence of other avenues of fast dye entry.

There are several lines of evidence implicating P2X-family ATP receptors as alternative means of dye permeation. Expression of $P2X_2$ receptors in a cell line has been shown to confer FM1-43 permeability (Meyers et al., 2003). Likewise, application of ATP to frog saccular hair cells increases their FM1-43 accumulation (MacDonald, 2002, Ph.D. thesis). The organ of Corti of mammals, the analogous structure to the chick basilar papilla, releases ATP into its extracellular environment (Zhao et al., 2005), thus hair cells are potentially exposed to an endogenous ligand for P2X receptors. Several P2X receptor subunits are expressed in mammalian hair cells, but expression in the chick inner ear has yet to be described, although chick hair cells show ATP-induced current and Ca^{2+} responses (Shigemoto and Ohmori, 1990). $P2X_{1,\ 2,\ 3,\ 4}$, and $_7$ are in mammalian hair cells, with $P2X_3$ primarily expressed early in development (Szucs et al., 2004, Huang et al., 2006). Four P2X receptor subunits have been cloned from chicken, including $P2X_1$, $P2X_4$, $P2X_5$, and the novel isoform $P2X_8$ (Bo et al., 2000, Bo et al., 2001, Ruppelt et al., 2001, Soto et al., 2003). A predicted sequence for chick $P2X_7$ is present in Genbank, but this putative homolog has not been independently cloned from native chick tissues. Transcripts for chick $P2X_2$, $P2X_3$, and $P2X_6$ have yet to be reported. We performed PCR using chick sensory epithelium to identify the purinergic receptor transcripts expressed in the basilar papilla. Primers to chick $P2X_{1,\ 4,\ 5}$, and $_8$ (Table 1) were designed based on published sequences. Gene products encoding each of these receptor subunits were found (Figure 3A), with each primer set producing a band of the expected size (Table 1). Although more work is required to fully understand purinergic signaling in the chick cochlea, these results indicate that the chick sensory epithelium expresses P2X-family receptor subunits.

These subunits, or other homologs that have yet to be found, may contribute to dye-uptake if ATP is natively available to stimulate them.

A luciferin-luciferase reporter assay was employed to assess the amount of ATP released from acutely dissected chick basilar papillae. Serially diluted ATP standards were used to calibrated the detection system, which had a linear response down to 20 pM ATP (Figure 3B). Saline bathing the dissected tissue was sampled three times at 5-minute intervals to detect immediate and sustained ATP release from the basilar papillae. Chemiluminescent measurement of these saline samples revealed that ATP is released from the chick basilar papilla, producing nanomolar concentrations in the bulk saline (Figure 3B). Repeated measures from separate incubations in fresh saline gave statistically similar concentrations, indicating that the papillae steadily release ATP into the external solution, similar to results from guinea pig cochlea reported elsewhere (Zhao et al., 2005). The measured concentration reflects the total of the ATP accumulated at the release site and the ATP that steadily diffused into the solution. Therefore, the local concentration at the tissue was likely much higher than the concentration measured in the bulk saline. We estimated the local concentration of ATP by calculating the accumulation in a 100-μm thick cylindrical disk at the bottom of the reaction tube (i.e. near the tissue) using the one-dimensional diffusion equation described in Experimental Procedures. The local concentration for the experimental conditions in the luciferin-luciferase assay was estimated as 6.2 μM. For the AM1-43 dye loading studies, accumulation over 1 minute for a single papilla was estimated to achieve a local concentration of 2.4 μM. These estimates are on par with the concentrations that activate cloned P2X receptors (North and Surprenant, 2000) and ATP currents in hair cells (Nakagawa et al., 1990, Yu and Zhao, 2008). Thus, ATP was available for the stimulation of P2X receptors in the basilar papilla.

Consistent with the observations of ATP release and P2X receptor expression, drugs that block P2X receptors were effective in decreasing hair cell uptake of AM1-43. Compounds tested were PPADS, suramin, TNP-ATP, and d-tubocurarine, all of which have inhibitory actions on P2X receptors (Glowatzki et al., 1997, Burgard et al., 2000, Li, 2000, Surprenant et al., 2000, Trujillo et al., 2006). Blocker dependent action on dye uptake was assessed by pre-incubating the chick basilar papilla with the antagonist for 5 minutes, then applying AM1-43 in the presence of the drug. PPADS (100 μM) decreased AM1-43 fluorescence by 69% (Figure 4A and B). Suramin (100 μM) was comparably effective, blocking 85% of the dye signal in hair cells. The compound TNP-ATP can be used to distinguish between receptors incorporating $P2X_1$ or $P2X_3$ subunits and those possessing only $P2X_2$, $P2X_4$, or $P2X_7$ subunits (Virginio et al., 1998). A concentration of 1 μM completely blocks $P2X_1$- or $P2X_3$-containing receptors, while 100 μM or more is necessary to block receptors comprised of only $P2X_2$, $P2X_4$, or $P2X_7$ subunits. In the dye assay, the difference in fluorescence between 1 μM TNP-ATP and control was statistically insignificant, while 100 μM TNP-ATP was as effective as PPADS and suramin at blocking dye entry (Figure 5A). The TNP-ATP data suggest that a pathway for AM1-43 entry is through homomeric $P2X_2$, $P2X_4$, or $P2X_7$ receptors. In light of the effects of PPADS and suramin, which have IC_{50}s in the 50-500 μM range for $P2X_4$ and $P2X_7$ receptors (North and Surprenant, 2000), the pharmacology points toward the involvement of a $P2X_2$ or a $P2X_2$-like receptor.

The actions of PPADS, suramin, and TNP-ATP on mechanotransduction are currently unknown, leaving the possibility that these blockers inhibited dye entry through transduction channels. However, the effect of another compound, tubocurarine, on both hair cell transduction and $P2X_2$ receptor currents has been previously evaluated. In turtle auditory hair cells, tubocurarine completely blocks mechanotransduction at a concentration of 100 μM (Farris et al., 2004). Likewise, in mouse outer hair cells, 100 μM blocks the transduction current, while it spares about 50–60% of ATP-activated current. At least 1 mM is needed to block nearly all of the ATP-induced currents. The dose-response curve for blockade of ATP-

induced currents in mouse hair cells is identical to the curve seen in xenopus oocytes expressing $P2X_2$, strongly suggesting that ATP-induced currents in mouse hair cells are mediated by homomeric $P2X_2$ receptors. Therefore, tubocurarine can be used to distinguish between an effect on mechanotransduction channels versus $P2X_2$ or $P2X_2$-like receptors. With 200 μM d-tubocurarine, there was no statistically significant difference in the loading of chick hair cells with AM1-43, compared to the control condition (Figure 5B). However, 2 mM d-tubocurarine decreased hair cell fluorescence by 72%, which is similar to the effect of the other P2X antagonists described above. The implication is that dye entry was preserved when transduction was blocked but substantially impeded when d-tubocurarine was concentrated enough to block $P2X_2$ receptors. Therefore, it appears that $P2X_2$ or a $P2X_2$-like receptor can mediate the entry of AM1-43 into chick hair cells.

Permeability to the large dye molecule, ethidium bromide, is sometimes induced through activation of pannexin hemichannels upon stimulation of $P2X_7$ receptors (Pelegrin and Surprenant, 2006). Finding that P2X antagonists significantly decreased the entry of AM1-43, we explored the involvement of secondary activation of pannexin hemichannels in the dye-loading of hair cells. Using PCR primers for pannexin-1, -2, and -3, we probed the isolated sensory epithelium of the chick cochlea for the three pannexin subtypes. All three subtypes were detected, indicating expression in hair cells or supporting cells (Figure 6A). Therefore, pannexins could play a role in the P2X-mediated entry of AM1-43. To test this possibility, we used 100 μM CBX, which is capable of blocking both connexin and pannexin hemichannels at this concentration (Bruzzone et al., 2005). Despite the presence of pannexin mRNA, treatment of the basilar papilla with 100 μM CBX failed to significantly decrease AM1-43 uptake by hair cells (Figure 6B). Considering that the tissue for the CBX experiment was pretreated longer than the tissue for the P2X antagonist experiments (1 hour vs. 5 min pretreatment), the controls for CBX and PPADS/suramin were compared (Figure 6B). The lack of CBX effect could have been due to diminished dye entry through a CBX-sensitive route over time. The dye loading of both control groups, however, was the same, so it appears unlikely that time affected the mechanism of dye loading. While we cannot rule out the participation of CBX-insentive hemichannels, the absence of a detectable CBX effect gives credence to the idea that the P2X antagonists prevented influx of dye flowing through the channels of P2X receptors, rather than through secondarily activated pannexin hemichannels.

Discussion

The evidence that styryl dyes rapidly enter hair cells though transduction channels is compelling. The most straight-forward support for the involvement of transduction channels comes from experiments where fluorescence was visualized during dye application. In frog sacular hair cells, loading with FM1-43 when the dye is streamed over the apical epithelial surface occurs only when the flow of dye deflects the hair bundles in the excitatory direction (i.e., the direction that opens transduction channels, Meyers et al., 2003). This kind of mechanical sensitivity is a hallmark of hair cell transduction channel function. The pattern of dye accumulation in hair cells further supports mechanotransducer channel involvement. The dye first enters the stereocilia and then progresses to the cell body, when the dye is applied to the apical epithelial surface of the organ of Corti (Gale et al., 2001, Meyers et al., 2003) or basilar papilla (Si et al., 2003). Likewise, focal application of dye to the tips of stereocilia causes a similar pattern (Meyers et al., 2003). Pharmacological evidence is also consistent with transduction channels acting as an intermediary for dye loading. For example, BAPTA or EGTA pretreatment has decreased the loading of hair cells with dye (Gale et al., 2001, Meyers et al., 2003). Aminoglycoside antibiotics and Gd^{3+}, which are known transduction blockers (Kroese et al., 1989, Kimitsuki et al., 1996), displayed good efficacy in preventing styryl dye uptake (Geleoc and Holt, 2003, Meyers et al., 2003, Cheatham et al., 2004). Finally, genetics also suggest transduction channel involvement, because dye accumulation is prevented in hair

cells with a mutation in myosin VIIa that shifts the activation range of transduction so that there is no current in the resting hair bundle (Gale et al., 2001). Taken together, these results suggest that styryl dyes enter hair cells via transduction channels, but it is difficult to conclude from these data that the dyes flow only through this pathway.

For nearly every piece of evidence above in favor of the role of transduction, there is a point of concern that casts doubt on this interpretation when P2X receptors are considered. The flow of dye from stereocilia to the cell body when it enters the cell could be produced by P2X receptors, due to their localization on the stereocilia. The tip-link-breaking actions of BAPTA and EGTA make them robust inhibitors of transduction, but these compounds chelate calcium, which could have affected a number of calcium-dependent processes. Moreover, EGTA and BAPTA eliminate only about half the dye signal (in this paper and Meyers et al., 2003), despite virtually eliminating mechanotransduction. While aminoglycosides and Gd^{3+} act as transduction channel blockers, aminoglycosides can block ATP-activated currents in hair cells (Lin et al., 1993) and Gd^{3+} blocks P2X receptors (Nakazawa et al., 1997). Finally, it is unknown if the mutation in myosin VIIa affects the activity of other channels, but the presence of myosin VIIa throughout hair cells suggests that non-transduction related functions could be disrupted by the mutation. The sensitivity of dye loading to the direction of hair bundle movement remains as strong evidence in support of transduction channels. However, the other evidence is equivocal, possibly reflecting a contribution by P2X receptors.

In the current report, we present evidence that AM1-43 can enter hair cells rapidly through a P2X-mediated route, activated by endogenously released ATP. While EGTA pretreatment decreased dye loading, drugs that block P2X receptors were more effective. Pannexin hemichannels have been implicated in the entry of the large dye molecules, ethidium bromide and YO-PRO-1, into cells upon stimulation of P2X receptors. Although we found that the chick basilar papilla expresses pannexins, we detected no effect of CBX, a drug that blocks pannexin pores. Therefore, we postulate that AM1-43 can enter hair cells directly through P2X receptors, rather than through a secondary mechanism involving pannexins.

An alternative explanation of the results is that the P2X antagonists had their effects on hair cell dye accumulation by blocking transduction channels. Indeed, there is evidence of overlapping pharmacology between transduction and P2X channels. For example, amiloride, neomycin, and the aforementioned d-tubocurarine, all compounds that are transduction channel inhibitors (Ohmori, 1985, Jorgensen and Ohmori, 1988, Housley et al., 1992, Glowatzki et al., 1997), also block ATP gated currents in hair cells (Housley et al., 1992, Lin et al., 1993, Glowatzki et al., 1997). It is conceivable that PPADS and suramin, both non-competitive P2X receptor antagonists, also inhibit transduction channels, although suramin reportedly does not affect putative standing transduction channel current remaining after tip-link loss (Meyer et al., 1998). Cross-pharmacology is a possibility for TNP-ATP as well, considering that it has been observed to inhibit voltage-gated sodium and potassium currents and currents through 5-HT_3 and N-methyl-D-aspartate receptors (Surprenant et al., 2000). For d-tubocurarine, however, we were able to take advantage of the separation between its inhibition of transduction and ATP-receptor currents in hair cells to tease apart effects at the two sites. At a concentration that blocks transduction current but preserves about half of the ATP-induced current, the mean intensity of dye signal was slightly less than control, but this difference was not statistically significant. It was only when the concentration of tubocurarine was high enough to block both types of current that AM1-43 uptake was prevented. This suggests that the AM1-43 entry into hair cells was dependent primarily on P2X receptors under our experimental conditions, with no explicit hair bundle stimulation.

There was substantial variability in the intensity of dye signal between papillae under control conditions (see Figure 4B, for example) that might reflect differential activation of P2X

receptors caused by the level of ATP release. Factors such as the degree of tissue perturbation and length of time to remove the tissue from the animal could have influenced the degree to which P2X receptors were activated by tissue ATP release and how much the receptors contribute to dye entry. Therefore, if using styryl dyes such as AM1-43 or FM1-43 as probes for hair cell mechanotransduction, the degree of ATP release and P2X receptor activation should be carefully considered. Under some circumstances, there might be little or no contribution by ATP-gated channels. For example, with isolated hair cells, extracellular ATP might be washed away and remain absent without a source of ongoing release. In other situations, such as with the whole auditory epithelium used here, ATP released by supporting cells might strongly activate purinergic receptors of hair cells. Consequently, caution must be exercised in concluding that rapid loading of hair cells with styryl dyes indicates the activity of hair cell transduction channels. Such an interpretation is made more sound if rapid dye loading were to be blocked by highly selective transduction channel antagonists, which are currently unavailable. Failing that, rapid styryl dye uptake in the absence of explicit mechanical stimulation of the hair bundle only indicates that some dye-permeable channel type is active. These additional channels should be taken into account, at least in part by examining the effects of P2X receptor antagonists. The results highlight the importance of developing better mechanotransduction channel antagonists and the complexity of using styryl dyes to indicate activity of those channels.

Acknowledgments

Supported by NIH-NIDCD Postdoctoral NRSA fellowship, F32-DC008050 (M.A.C.), generous support from the University of Michigan Department of Otolaryngology (R.K.D.), NIH-NIDCD grant R01-DC007432 (R.K.D.), and NIH-NIDCD Core grant, P30-DC05188. The authors thank Susan Shore for the use of equipment, Karl Grosh for guidance in the estimation of local ATP concentration, and Yehoash Raphael for comments on the manuscript and further support (NIH-NIDCD grant R01-DC01634).

List of abbreviations used in the main text

CBX	carbenoxolone
EGTA	ethylene glycol-bis(2-aminoethylether)-*N*,*N*,*N*′, *N*′-tetraacetic acid
LCHBSS	low calcium Hanks' Balanced Salt Solution
PBS	phosphate buffered saline
PPADS	pyridoxalphosphate-6-azophenyl-2′,4′-disulfonic acid
SEM	standard error of the mean
TNP-ATP	2′,3′-O-(2,4,6-Trinitrophenyl) adenosine 5′-triphosphate

Literature Cited

Betz WJ, Bewick GS. Optical analysis of synaptic vesicle recycling at the frog neuromuscular junction. Science 1992;255:200–203. [PubMed: 1553547]

Betz WJ, Mao F, Bewick GS. Activity-dependent fluorescent staining and destaining of living vertebrate motor nerve terminals. J Neurosci 1992;12:363–375. [PubMed: 1371312]

Bo X, Schoepfer R, Burnstock G. Molecular cloning and characterization of a novel ATP P2X receptor subtype from embryonic chick skeletal muscle. J Biol Chem 2000;275:14401–14407. [PubMed: 10799522]

Bo XN, Liu M, Schoepfer R, Burnstock G. Characterization and expression of ATP P2X(4) receptor from embryonic chick skeletal muscle. Drug Development Research 2001;53:22–28.

Bruzzone R, Barbe MT, Jakob NJ, Monyer H. Pharmacological properties of homomeric and heteromeric pannexin hemichannels expressed in Xenopus oocytes. J Neurochem 2005;92:1033–1043. [PubMed: 15715654]

Burgard EC, Niforatos W, van Biesen T, Lynch KJ, Kage KL, Touma E, Kowaluk EA, Jarvis MF. Competitive antagonism of recombinant P2X(2/3) receptors by 2′, 3′-O-(2,4,6-trinitrophenyl) adenosine 5′-triphosphate (TNP-ATP). Mol Pharmacol 2000;58:1502–1510. [PubMed: 11093790]

Chaumont S, Khakh BS. Patch-clamp coordinated spectroscopy shows P2X2 receptor permeability dynamics require cytosolic domain rearrangements but not Panx-1 channels. Proc Natl Acad Sci U S A 2008;105:12063–12068. [PubMed: 18689682]

Cheatham MA, Huynh KH, Gao J, Zuo J, Dallos P. Cochlear function in Prestin knockout mice. J Physiol 2004;560:821–830. [PubMed: 15319415]

Choi SY, Borghuis BG, Rea R, Levitan ES, Sterling P, Kramer RH. Encoding light intensity by the cone photoreceptor synapse. Neuron 2005;48:555–562. [PubMed: 16301173]

Crawford AC, Evans MG, Fettiplace R. The actions of calcium on the mechano-electrical transducer current of turtle hair cells. J Physiol 1991;434:369–398. [PubMed: 1708822]

Doyle KL, Kazda A, Hort Y, McKay SM, Oleskevich S. Differentiation of adult mouse olfactory precursor cells into hair cells in vitro. Stem Cells 2007;25:621–627. [PubMed: 17110620]

Duncan RK, Dyce OH, Saunders JC. Low calcium abolishes tip links and alters relative stereocilia motion in chick cochlear hair cells. Hear Res 1998;124:69–77. [PubMed: 9822903]

Farris HE, LeBlanc CL, Goswami J, Ricci AJ. Probing the pore of the auditory hair cell mechanotransducer channel in turtle. J Physiol 2004;558:769–792. [PubMed: 15181168]

Gale JE, Marcotti W, Kennedy HJ, Kros CJ, Richardson GP. FM1-43 dye behaves as a permeant blocker of the hair-cell mechanotransducer channel. J Neurosci 2001;21:7013–7025. [PubMed: 11549711]

Geleoc GS, Holt JR. Developmental acquisition of sensory transduction in hair cells of the mouse inner ear. Nat Neurosci 2003;6:1019–1020. [PubMed: 12973354]

Glowatzki E, Ruppersberg JP, Zenner HP, Rusch A. Mechanically and ATP-induced currents of mouse outer hair cells are independent and differentially blocked by d-tubocurarine. Neuropharmacology 1997;36:1269–1275. [PubMed: 9364481]

Griesinger CB, Richards CD, Ashmore JF. Fm1-43 reveals membrane recycling in adult inner hair cells of the mammalian cochlea. J Neurosci 2002;22:3939–3952. [PubMed: 12019313]

Griesinger CB, Richards CD, Ashmore JF. Apical endocytosis in outer hair cells of the mammalian cochlea. Eur J Neurosci 2004;20:41–50. [PubMed: 15245477]

Hazel JR, Sidell BD. A method for the determination of diffusion coefficients for small molecules in aqueous solution. Anal Biochem 1987;166:335–341. [PubMed: 3434777]

Housley GD, Greenwood D, Ashmore JF. Localization of cholinergic and purinergic receptors on outer hair cells isolated from the guinea-pig cochlea. Proc Biol Sci 1992;249:265–273. [PubMed: 1359556]

Housley GD, Kanjhan R, Raybould NP, Greenwood D, Salih SG, Jarlebark L, Burton LD, Setz VC, Cannell MB, Soeller C, Christie DL, Usami S, Matsubara A, Yoshie H, Ryan AF, Thorne PR. Expression of the P2X(2) receptor subunit of the ATP-gated ion channel in the cochlea: implications for sound transduction and auditory neurotransmission. J Neurosci 1999;19:8377–8388. [PubMed: 10493739]

Housley GD, Raybould NP, Thorne PR. Fluorescence imaging of Na+ influx via P2X receptors in cochlear hair cells. Hear Res 1998;119:1–13. [PubMed: 9641314]

Hu Z, Corwin JT. Inner ear hair cells produced in vitro by a mesenchymal-to-epithelial transition. Proc Natl Acad Sci U S A 2007;104:16675–16680. [PubMed: 17895386]

Huang LC, Ryan AF, Cockayne DA, Housley GD. Developmentally regulated expression of the P2X3 receptor in the mouse cochlea. Histochem Cell Biol 2006;125:681–692. [PubMed: 16341871]

Jarlebark LE, Housley GD, Thorne PR. Immunohistochemical localization of adenosine 5′-triphosphate-gated ion channel P2X(2) receptor subunits in adult and developing rat cochlea. J Comp Neurol 2000;421:289–301. [PubMed: 10813788]

Jorgensen F, Ohmori H. Amiloride blocks the mechano-electrical transduction channel of hair cells of the chick. J Physiol 1988;403:577–588. [PubMed: 2473197]

Kaneko T, Harasztosi C, Mack AF, Gummer AW. Membrane traffic in outer hair cells of the adult mammalian cochlea. Eur J Neurosci 2006;23:2712–2722. [PubMed: 16817874]

Kimitsuki T, Nakagawa T, Hisashi K, Komune S, Komiyama S. Gadolinium blocks mechano-electric transducer current in chick cochlear hair cells. Hear Res 1996;101:75–80. [PubMed: 8951434]

Kroese AB, Das A, Hudspeth AJ. Blockage of the transduction channels of hair cells in the bullfrog's sacculus by aminoglycoside antibiotics. Hear Res 1989;37:203–217. [PubMed: 2468634]

Li C. Novel mechanism of inhibition by the P2 receptor antagonist PPADS of ATP-activated current in dorsal root ganglion neurons. J Neurophysiol 2000;83:2533–2541. [PubMed: 10805655]

Lin X, Hume RI, Nuttall AL. Voltage-dependent block by neomycin of the ATP-induced whole cell current of guinea-pig outer hair cells. J Neurophysiol 1993;70:1593–1605. [PubMed: 7506758]

MacDonald, RB. Gentamicin and FM1-43 enter sensory hair cells through the mechanosensory transduction channel. United States -- Massachusetts: Massachusetts Institute of Technology; 2002.

Marquis RE, Hudspeth AJ. Effects of extracellular Ca2+ concentration on hair-bundle stiffness and gating-spring integrity in hair cells. Proc Natl Acad Sci U S A 1997;94:11923–11928. [PubMed: 9342338]

Mei, CC. Mathematical analysis in engineering: How to use the basic tools. Cambridge, United Kingdom: Cambridge University Press; 1997.

Meyer J, Furness DN, Zenner HP, Hackney CM, Gummer AW. Evidence for opening of hair-cell transducer channels after tip-link loss. J Neurosci 1998;18:6748–6756. [PubMed: 9712646]

Meyer J, Mack AF, Gummer AW. Pronounced infracuticular endocytosis in mammalian outer hair cells. Hear Res 2001;161:10–22. [PubMed: 11744276]

Meyers JR, MacDonald RB, Duggan A, Lenzi D, Standaert DG, Corwin JT, Corey DP. Lighting up the senses: FM1-43 loading of sensory cells through nonselective ion channels. J Neurosci 2003;23:4054–4065. [PubMed: 12764092]

Munoz DJ, Kendrick IS, Rassam M, Thorne PR. Vesicular storage of adenosine triphosphate in the guinea-pig cochlear lateral wall and concentrations of ATP in the endolymph during sound exposure and hypoxia. Acta Otolaryngol 2001;121:10–15. [PubMed: 11270486]

Munoz DJ, Thorne PR, Housley GD, Billett TE. Adenosine 5′-triphosphate (ATP) concentrations in the endolymph and perilymph of the guinea-pig cochlea. Hear Res 1995;90:119–125. [PubMed: 8974988]

Nakagawa T, Akaike N, Kimitsuki T, Komune S, Arima T. ATP-induced current in isolated outer hair cells of guinea pig cochlea. J Neurophysiol 1990;63:1068–1074. [PubMed: 2358862]

Nakazawa K, Liu M, Inoue K, Ohno Y. Potent inhibition by trivalent cations of ATP-gated channels. Eur J Pharmacol 1997;325:237–243. [PubMed: 9163571]

Nishikawa S, Sasaki F. Internalization of styryl dye FM1-43 in the hair cells of lateral line organs in Xenopus larvae. J Histochem Cytochem 1996;44:733–741. [PubMed: 8675994]

North RA, Surprenant A. Pharmacology of cloned P2X receptors. Annu Rev Pharmacol Toxicol 2000;40:563–580. [PubMed: 10836147]

Ohmori H. Mechano-electrical transduction currents in isolated vestibular hair cells of the chick. J Physiol 1985;359:189–217. [PubMed: 2582113]

Pelegrin P, Surprenant A. Pannexin-1 mediates large pore formation and interleukin-1beta release by the ATP-gated P2X7 receptor. EMBO J 2006;25:5071–5082. [PubMed: 17036048]

Ricci AJ, Crawford AC, Fettiplace R. Tonotopic variation in the conductance of the hair cell mechanotransducer channel. Neuron 2003;40:983–990. [PubMed: 14659096]

Ruppelt A, Ma W, Borchardt K, Silberberg SD, Soto F. Genomic structure, developmental distribution and functional properties of the chicken P2X(5) receptor. J Neurochem 2001;77:1256–1265. [PubMed: 11389176]

Shigemoto T, Ohmori H. Muscarinic agonists and ATP increase the intracellular Ca2+ concentration in chick cochlear hair cells. J Physiol 1990;420:127–148. [PubMed: 2324982]

Si F, Brodie H, Gillespie PG, Vazquez AE, Yamoah EN. Developmental assembly of transduction apparatus in chick basilar papilla. J Neurosci 2003;23:10815–10826. [PubMed: 14645474]

Soto F, Krause U, Borchardt K, Ruppelt A. Cloning, tissue distribution and functional characterization of the chicken P2X1 receptor. FEBS Lett 2003;533:54–58. [PubMed: 12505158]

Spencer NJ, Cotanche DA, Klapperich CM. Peptide- and collagen-based hydrogel substrates for in vitro culture of chick cochleae. Biomaterials 2008;29:1028–1042. [PubMed: 18037163]

Stepanyan R, Belyantseva IA, Griffith AJ, Friedman TB, Frolenkov GI. Auditory mechanotransduction in the absence of functional myosin-XVa. J Physiol 2006;576:801–808. [PubMed: 16973713]

Surprenant A, Schneider DA, Wilson HL, Galligan JJ, North RA. Functional properties of heteromeric P2X(1/5) receptors expressed in HEK cells and excitatory junction potentials in guinea-pig submucosal arterioles. J Auton Nerv Syst 2000;81:249–263. [PubMed: 10869729]

Szucs A, Szappanos H, Toth A, Farkas Z, Panyi G, Csernoch L, Sziklai I. Differential expression of purinergic receptor subtypes in the outer hair cells of the guinea pig. Hear Res 2004;196:2–7. [PubMed: 15464295]

Taura A, Kojima K, Ito J, Ohmori H. Recovery of hair cell function after damage induced by gentamicin in organ culture of rat vestibular maculae. Brain Res 2006;1098:33–48. [PubMed: 16764839]

Tritsch NX, Yi E, Gale JE, Glowatzki E, Bergles DE. The origin of spontaneous activity in the developing auditory system. Nature 2007;450:50–55. [PubMed: 17972875]

Trujillo CA, Nery AA, Martins AH, Majumder P, Gonzalez FA, Ulrich H. Inhibition mechanism of the recombinant rat P2X(2) receptor in glial cells by suramin and TNP-ATP. Biochemistry 2006;45:224–233. [PubMed: 16388598]

Virginio C, MacKenzie A, Rassendren FA, North RA, Surprenant A. Pore dilation of neuronal P2X receptor channels. Nat Neurosci 1999;2:315–321. [PubMed: 10204537]

Virginio C, Robertson G, Surprenant A, North RA. Trinitrophenyl-substituted nucleotides are potent antagonists selective for P2X1, P2X3, and heteromeric P2X2/3 receptors. Mol Pharmacol 1998;53:969–973. [PubMed: 9614197]

Vollrath MA, Kwan KY, Corey DP. The micromachinery of mechanotransduction in hair cells. Annu Rev Neurosci 2007;30:339–365. [PubMed: 17428178]

Yan Z, Li S, Liang Z, Tomic M, Stojilkovic SS. The P2X7 receptor channel pore dilates under physiological ion conditions. J Gen Physiol 2008;132:563–573. [PubMed: 18852304]

Yu N, Zhao HB. ATP activates P2x receptors and requires extracellular Ca(++) participation to modify outer hair cell nonlinear capacitance. Pflugers Arch. 2008

Zhao HB, Yu N, Fleming CR. Gap junctional hemichannel-mediated ATP release and hearing controls in the inner ear. Proc Natl Acad Sci U S A 2005;102:18724–18729. [PubMed: 16344488]

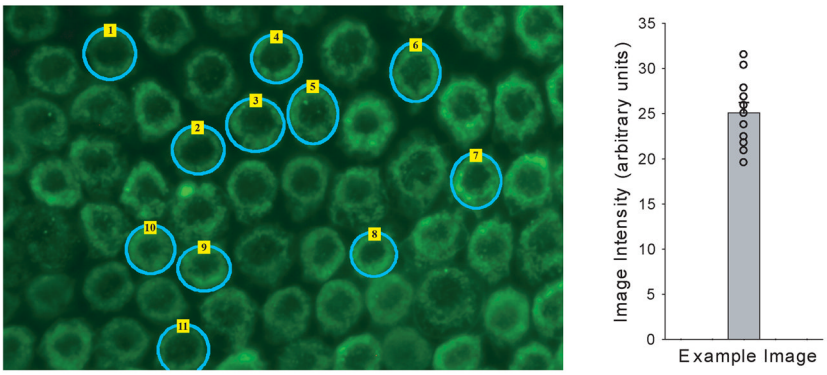

Figure 1. Measurement of AM1-43 fluorescence in hair cells

Eliptical regions of interest (ROIs) were drawn around representative hair cells for measuring fluorescence intensity. In order to be included in the analysis, ROIs had to include a single hair cell with clearly defined borders and a logitudinal axis that was parallel with the optical axis. Suitable ROIs were devoid of debris and label outside the focal plane. The outlines were drawn to encapsulate hair cells only. Care was taken to ensure that ROIs covered the full range of intensities exhibited by cells across the image. Each circle in the plot represents the fluorescence intensity of a cell in the example image. The bar represents the mean of the individual cell intensities (error bar = SEM), which is the fluorescence value for this piece of tissue.

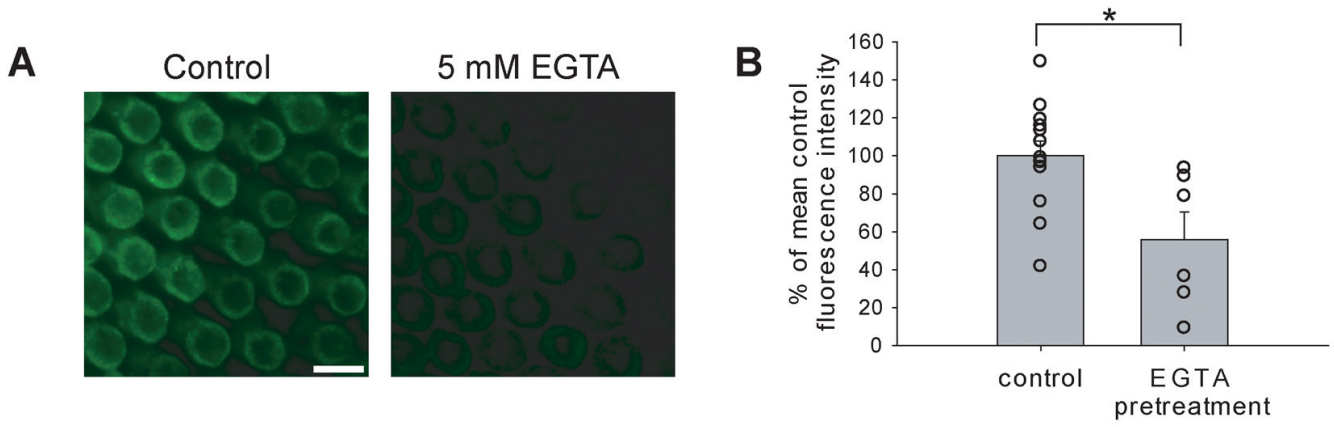

Figure 2. Partial block of AM1-43 entry into hair cells by EGTA

A. Example images of chick basilar papilla exposed to AM1-43 after pre-treatment with saline containing 5 mM EGTA or lacking EGTA (control). Scale bar represents 10 μm and applies to both images. B. Plot of AM1-43 fluorescence expressed as percent of the mean control value. Each circle represents the individual fluorescence value for a papilla. Bar graphs represent the mean of the papilla values for the experimental condition (error bars = SEM). Fluorescence was approximately halved by treatment with the tip-link breaker, EGTA. * $p < 0.05$.

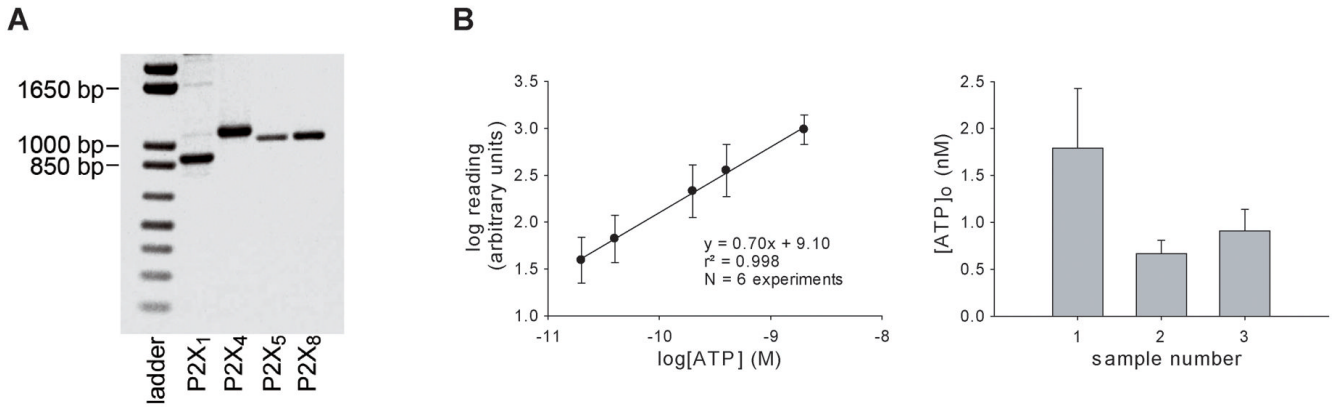

Figure 3. Basilar papilla P2X receptor expression and ATP release

A. PCR amplification was used to probe the chick sensory epithelium for expression of $P2X_{1, 4, 5}$, and $_8$. Bands at the expected sizes were found for all four isoforms (see Table 1). No bands were seen when dissection saline was assayed (data not shown). B. ATP was measured in the bathing solution of isolated basilar papillae by a chemiluminescent assay in order to determine if there is ATP released from this tissue. The left plot displays the mean ATP standard curve, demonstrating the linearity and sensitivity of the assay. The right plot shows the concentration of ATP accumulated in saline bathing two basilar papillae (n = 10 trials). The sample numbers represent successive 5-minute incubations of the same tissue in fresh saline. There were no statistically significant differences in $[ATP]_o$ between the samples. Error bars = SEM for both plots.

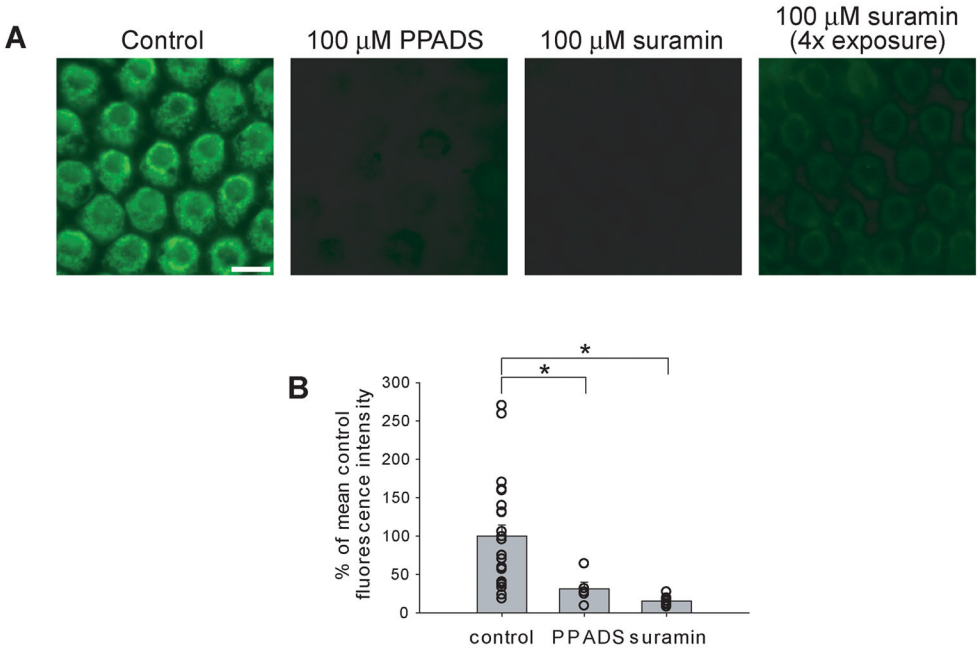

Figure 4. Effect of the P2X antagonists, PPADS and suramin, on AM1-43 entry

A. Example images of AM1-43 treated chick basilar papilla in the presence or absence (control) of P2X receptor antagonists. Fluorescence was essentially eliminated by both PPADS and suramin in these specimens. Both suramin images show the same area of the papilla, but the second image used a longer exposure to show that hair cells and a low level of fluorescence were present. Scale bar represents 10 μm and applies to all images. B. Plot of the effect of 100 μM PPADS and 100 μM suramin. Both PPADS and suramin blocked hair cell uptake of AM1-43 by at least 69%. The plot conventions are the same as in Figure 2B. * $p < 0.05$.

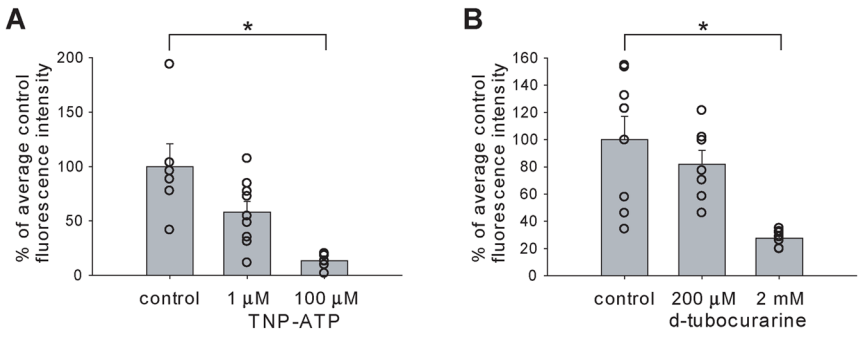

Figure 5. Pharmacological dissection of channel identity

A. The P2X antagonist, TNP-ATP, can be used to distinguish between receptors incorporating $P2X_1$ or $P2X_3$ subunits and those possessing only $P2X_2$, $P2X_4$, or $P2X_7$ subunits. At a concentration of 1 μM the difference compared to control was statistically insignificant, but at 100 μM hair cell fluorescence was decreased by 87%, indicating possible involvement of a homomeric $P2X_2$, $P2X_4$, or $P2X_7$ receptor. B. To distinguish between an effect on transduction channels versus P2X receptors, d-tubocurarine was used at 200 μM and 2 mM. The 2 mM concentration should block both transduction channels and $P2X_2$ receptors, while the 200 μM concentration should spare $P2X_2$ receptors. Only when $P2X_2$ receptors were spared (200 μM d-tubocurarine) was there substantial dye loading compared to control. The 2 mM concentration had a significant effect on fluorescence, decreasing it by 72%, suggesting a decrease in AM1-43 loading due to blockade of $P2X_2$-like receptors. The plot conventions are the same as in Figure 2B. * $p < 0.05$.

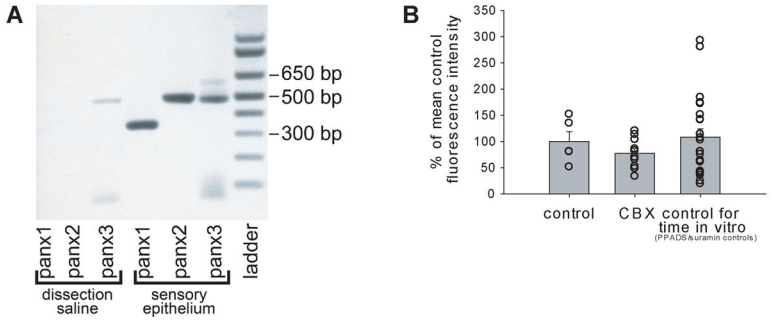

Figure 6. Pannexins and AM1-43 loading of hair cells

A. Pannexins-1, -2, and -3 were detected in isolated chick basilar papilla (sensory epithelium) by PCR amplification. For the sensory epithelial tissue, bands at the expected sizes were generated for all three isoforms (see Table 1). These bands were much more intense than those obtained from the dissection saline that contained the tissue, used as a control. B. Carbenoxolone (CBX, 100 μM), a blocker of pannexins and connexins, was ineffective at blocking AM1-43 uptake by hair cells. No statistically significant difference was detected between the fluorescence with CBX treatment and that of similarly handled control tissue. Since the pretreatment duration in this experiment (1 hour) was substantially longer than the pretreatment with the P2X drugs (5 min), the PPADS/suramin control data are shown for comparison, as a percentage of the CBX control. The fluorescence of this group was statistically indistinguishable from the CBX control. The plot conventions are the same as in Figure 2B.

Table 1

PCR primers for chick P2X and pannexin genes

Gene Name	Accession Number	Primer direction	Primer sequence	Expected size of PCR product
$P2X_1$	NM_204519	forward reverse	ACATCTGGGATGTGGTGGAT AAAATGCAGCAGGAGCAGAT	824 bp
$P2X_4$	NM_204291	forward reverse	TCCAGGATCTGGGATGTAGC ATCCGGTTCTCCTCTTTGGT	1058 bp
$P2X_5$	NM_204748	forward reverse	CAGACTTCGCTGGGTTCTTC CTGAAGCCCCTGAAGACTTG	997 bp
$P2X_8$	AF_205066	forward reverse	GCTACCCCAGATCAGATCCA GAAGAACCCAGCGAAGTCTG	1007 bp
Pannexin-1	XM_001235338	forward reverse	CTCACCTCTCTTCGGACCTG TGATGGTGCAGAGAAACTCG	348 bp
Pannexin-2	XM_424545	forward reverse	TTATGCACTGCTGGCTTTTG ATCCTCTGGAGCTGGACAGA	492 bp
Pannexin-3	XM_001231502	forward reverse	CTGCCCTTCACTCTGACCTC CTGCAGGGCACTGTAGATGA	479 bp